Supporting Information

Effects of point defects on the magnetoelectronic structures of MXenes from first principles

Structure and Energetics:

In all the Ti_2XT_2 systems, the X atoms are in perfect octahedral environment in an Oh symmetry, whereas, in case of Ti_2NO_2, N atom is in a D_{4h} symmetry, with two elongated Ti-N bonds. These Ti-N bonds again after defect formation becomes same in length locally.

We compared the energetics of the asymmetric and symmetric Ti_2NO_2 structures (where all the Ti-N and Ti-O bond lengths are same) and find that, asymmetric structure is 0.77 eV more stable. Plotting the charge density difference of the asymmetric and symmetric structure in Figure 2, we find that there is a gain of charge density on Ti-O bond in asymmetric Ti_2NO_2 structure, which gives rise to stronger Ti-O bond formation, leading to stable asymmetric structure. Also, in the symmetric structure the Ti-N bond lengths are 2.17 Å and Ti-O bond lengths are 1.99 Å, again suggesting two shorter and stronger Ti- or Ti-O bond formation in asymmetric Ti_2NO_2.

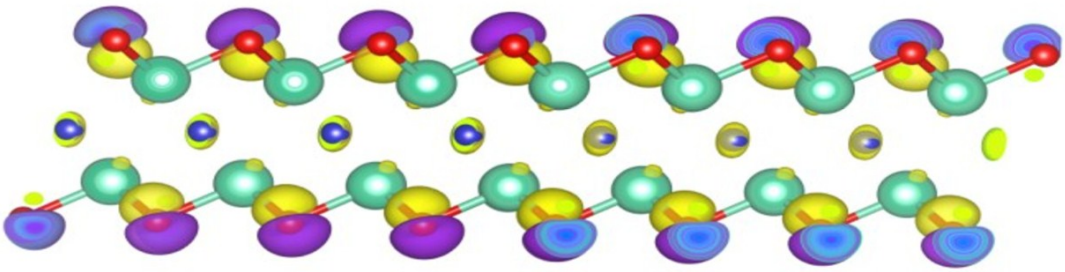

Figure S1: Charge density difference plot in Ti_2NO_2, yellow region denotes charge accumulation region and purple region denotes charge depletion region in asymmetric Ti_2NO_2 structure.

Table S1: Bond lengths and unit cell lengths of Ti_2XT_2 systems before and after single vacancy (SV) formation

System	Ti-X bond length (Å)		Ti-T bond length (Å)		Unit cell length (Å) a/b
	Pure	Near SV	Pure	Near SV	

		V_{Ti}	V_X	V_T		V_{Ti}	V_X	V_T	
Ti_2CO_2	2.19	2.16	2.18	2.19	1.98	1.85	1.95	1.95	3.04
Ti_2CF_2	2.10	2.07	2.10	2.11	2.16	2.02	2.14	2.14	3.06
$Ti_2C(OH)_2$	2.12	2.08	2.11	2.12	2.18	2.14	2.17	2.17	3.08
Ti_2NO_2	2.09 2.17	2.06 2.05	2.10	2.07 2.11	2.05 1.94	1.84	1.96 1.90	2.02 1.96	3.00
Ti_2NF_2	2.07	2.02	2.10	2.07	2.16	2.03	2.13	2.15	3.05
$Ti_2N(OH)_2$	2.08	2.08	2.11	2.08	2.17	2.12	2.14	2.16	3.05

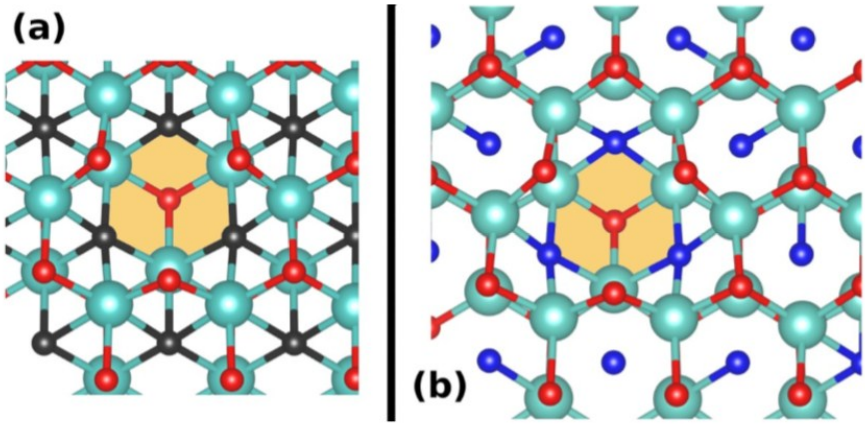

Figure S2: Structural reorganization in (a) V_C-Ti_2CO_2 and (b) V_N-Ti_2NO_2. This suggests Ti_2NO_2 exhibits more prominent changes because of X defect formation than Ti_2CO_2.

Magnetic Properties:

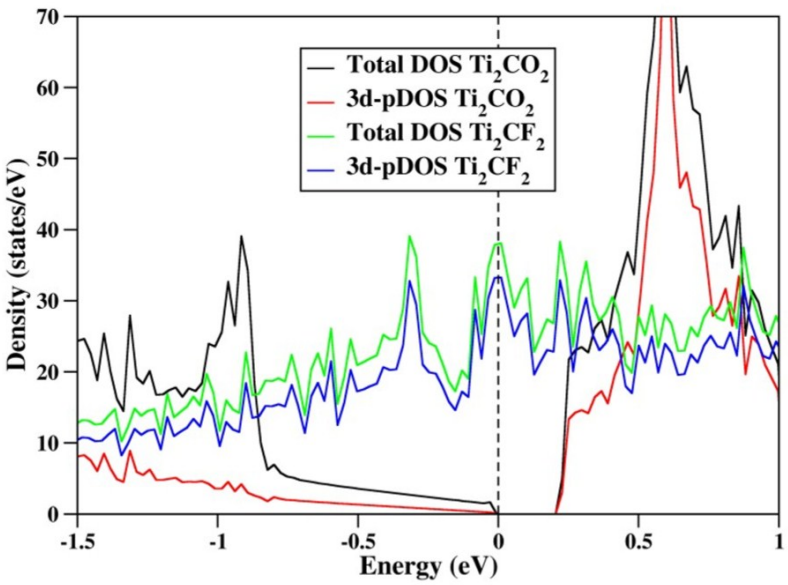

Figure S3: Projected density of states (pDOS) plots of Ti_2CO_2 and Ti_2CF_2, showing the contribution of 3d orbitals of Ti. It confirms Ti_2CF_2 has filled 3d orbitals but Ti_2CO_2 has vacant 3d orbital.

Electronic Properties:

Except Ti_2XO_2 systems, all the other systems are metallic in nature both in their pristine and defective form. Here we are giving band structure plots for two systems as example.

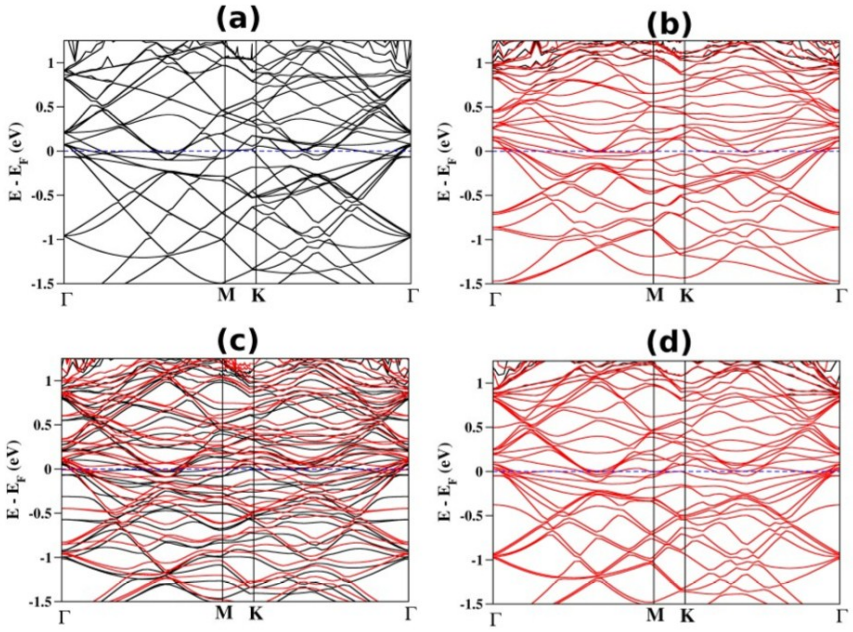

Figure S4: Band structure plot of (a) pure Ti_2CF_2, (b) V_{Ti}-Ti_2CF_2, (c) V_C-Ti_2CF_2 and (d) V_F-Ti_2CF_2

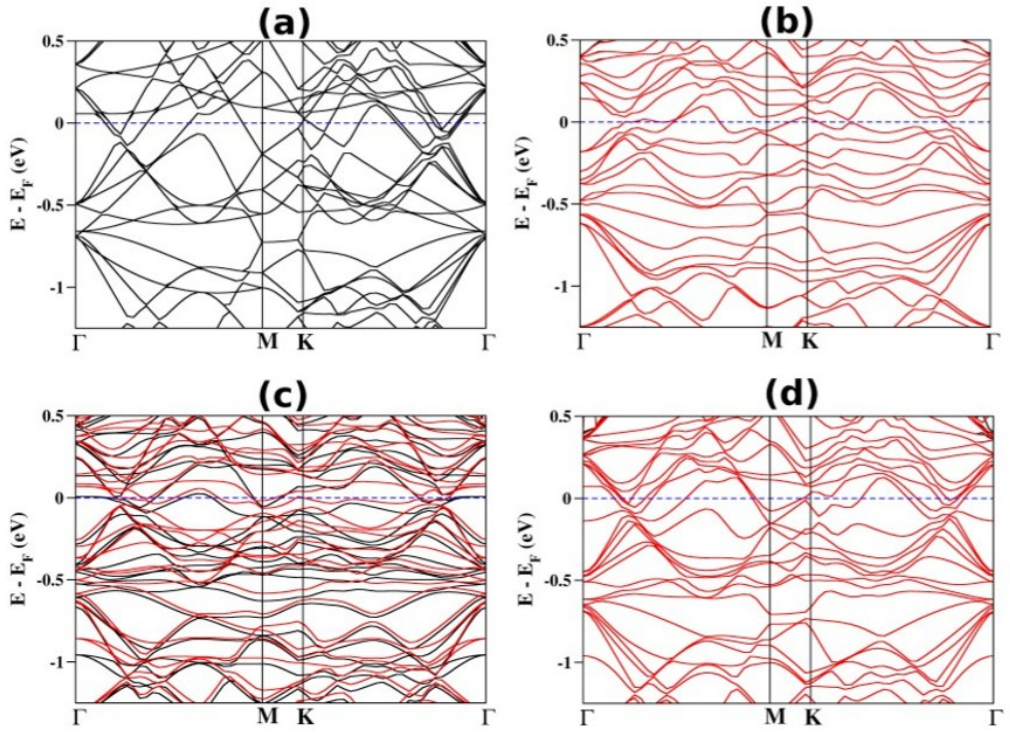

Figure S5: Band structure plot of (a) pure Ti_2NF_2, (b) V_{Ti}-Ti_2NF_2, (c) V_N-Ti_2NF_2 and (d) V_F-Ti_2NF_2

SV in Other MXenes:

To generalize our findings for defect formation in Ti_2XT_2, we have studied the defect formation mechanism in other transition metal atom containing MXenes, such as, V_2CO_2, Mn_2CO_2, Ta_2CO_2 and Re_2CO_2, also. Note that, all of these pure systems have been studied previously.[1-3] The formation energy of the SVs in V_2CO_2, Mn_2CO_2, Ta_2CO_2 and Re_2CO_2 follows the same trend as that of Ti_2CO_2 (see Table S2), that is M defect formation is more difficult than C defect formation. In these cases, M-O bond is stronger than M-C bonds, thus, breaking three M-C bonds and three M-O bonds requires more energy than breaking six M-C bonds, which leads to smaller C defect and higher M defect formation energies. For example, we have calculated the formation energy of the V-C and V-O bonds, and found that V-O bond energy is 3.4 eV and V-C bond energy is 1.71 eV. Similarly, Mn-O bond energy is 1.35 eV ad Mn-C bond energy is 0.49 eV. This also tells that in Mn_2CO_2, Mn and C SV formation energy difference is smaller than that of V_2CO_2. Thus, in these MXenes also, where other metal atoms are present, C defect formation is much easier than metal defect formation

because of the presence of a stronger M-O bond in the system validating our result for Ti_2XT_2 systems.

Table S2: SV formation energy in other MXenes:

System	Defect formation energy (eV)		
	M defect	C defect	O defect
V_2CO_2	3.44	0.74	3.08
Mn_2CO_2	3.15	1.06	1.09
Ta_2CO_2	6.42	3.06	5.08
Re_2CO_2	2.06	0.99	1.01

Schottky type defect:

Table S3: Schottky type defect formation energy for MXenes:

System	Defect formation energy (eV)			
	TiX defect (near)	TiX defect (distant)	TiO_2 defect (near)	TiO_2 defect (distant)
Ti_2CO_2	3.86	4.98	3.16	5.99
Ti_2NO_2	1.73	2.06	2.02	3.42

TiC/N defects inTi_2CF_2, $Ti_2C(OH)_2$, Ti_2NF_2 and $Ti_2N(OH)_2$ shows same trend, e.g., in Ti_2CF_2, TiC_{near} energy is 3.58 eV and $TiC_{distant}$ energy is 4.41 eV.

Born Oppenheimer Molecular Dynamics calculations:

To consider the reconstruction process in room temperature, we perform constant-temperature BOMD simulations considering the canonical ensemble (NVT) as implemented in the Vienna Ab initio Simulation Package (VASP). We have used the same parameters used for DFT calculations for BOMD calculations also, We use a Nose-Hoover thermostat to adjust the temperature at 300 K during the simulations, and we consider a time step of 1 fs to integrate the equation of motion.[4-6] We have run the simulation upto 40 ps.

Performing the BOMD simulation at 300 K and analysing the resulting trajectory, we find that the equilibrated structures do not show any kind reconstruction or healing process (see Figure S6). Interestingly, Ti_2NO_2, in room temperature also remain asymmetric in nature. The magnetic system V_C-Ti_2CF_2 retain its magnetic nature even in room temperature.

Moreover, we also have performed AIMD simulation with higher temperature, T=500K to access the probable higher energy barrier of structural transition for V_C-Ti_2CO_2 system. However, as shown in Fig S6, we find no signature of reconstruction of defects during 20 ps long simulation. With this, we can comment about the stability of defects at finite temperature with some certainty.

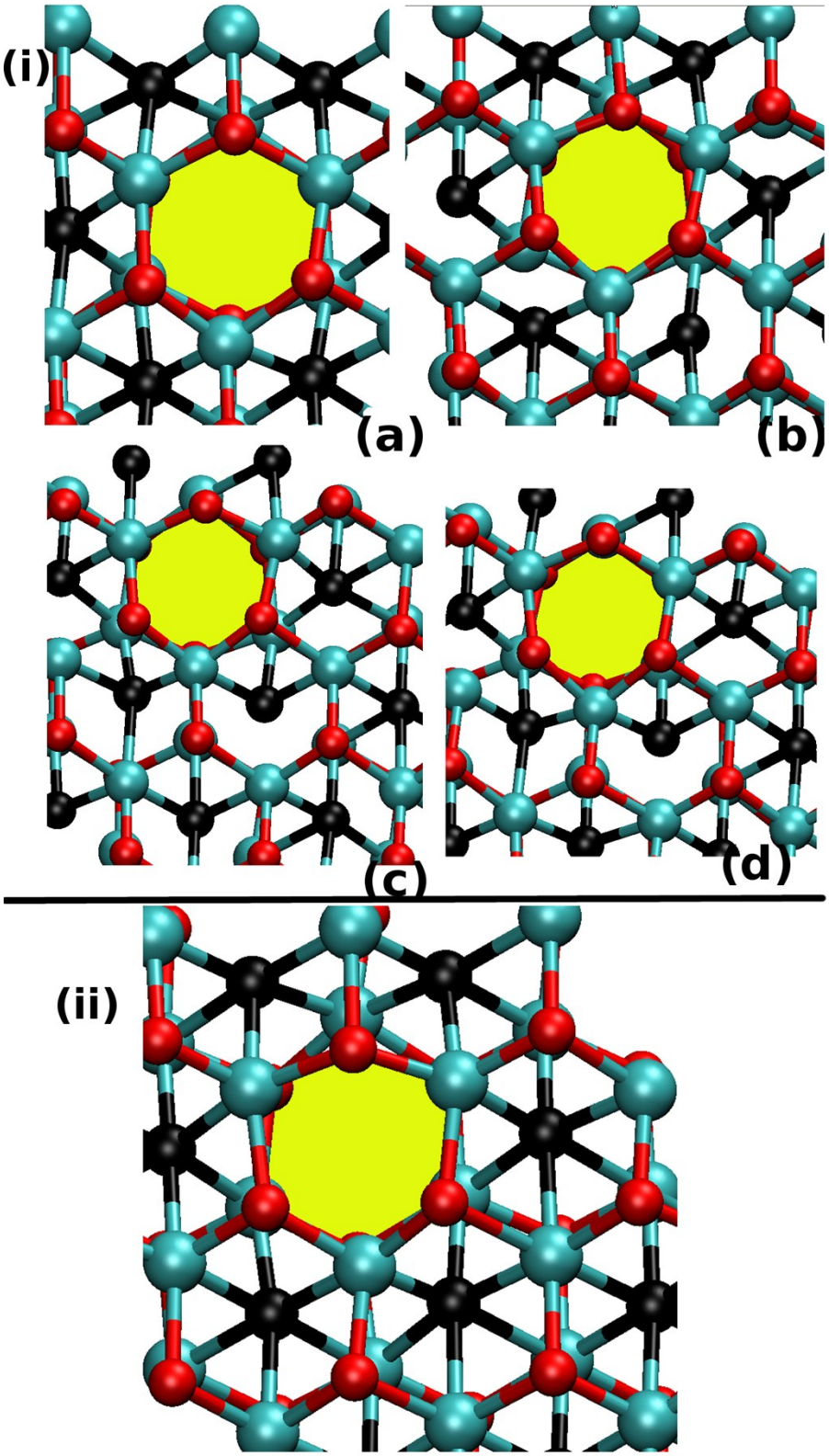

Figure S6 (i) 300 K simulation snapshots at (a) 25, (b) 30, (c) 35 and (d) 40 ps for C_V-Ti_2CO_2 and (ii)) 300 K simulation snapshots at 20 ps for C_V-Ti_2CO_2

We find that in presence of multiple defects (in our study Schottky or Frenkel type defects) also the electronic properties of a MXene layer change, as can be seen in Figure S7.

With Schottky and Frenkel type defects, the band-gap variation ensures metal-semiconductor transition in Ti_2CO_2. Schottky defect formation widens up the smaller band-gap of Ti_2CO_2 to 0.48 eV (TiO_2 defect) and 0.33 eV (TiC defect), whereas, the Frenkel type defect leads to semiconductor to metal transition in Ti_2CO_2.

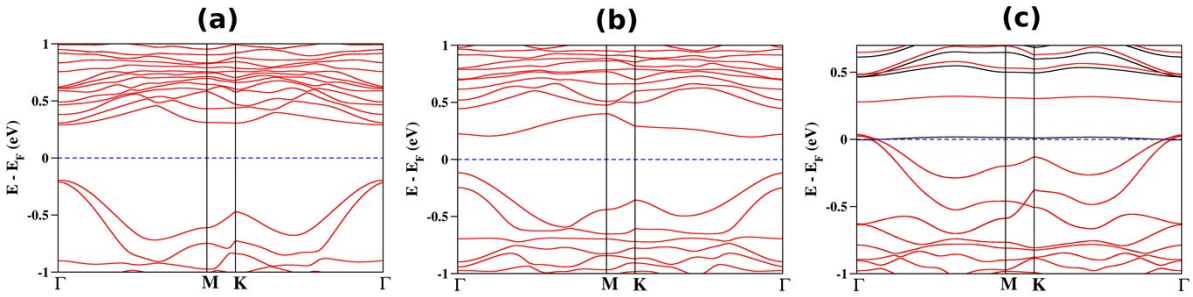

Figure S7: Band structure plot for TiO_2 defect, TiC defect and a frenkel type defect in Ti_2CO_2.

Oxidation State:

In our calculations, we have compared the well-known TiC or TiO2, which is in +4 formal oxidation state, with our Ti_2CO_2 system in the same lavel of theory and found similar bader charge on Ti atom for all of them. As our system is not completely ionic, Ti shows a presence of fractional amount of electron in its d-orbital, but this amount is negligible compared to Ti_2CF_2 or $Ti_2C(OH)_2$ (as can be seen in Figure S8), thus our results remain unaltered.

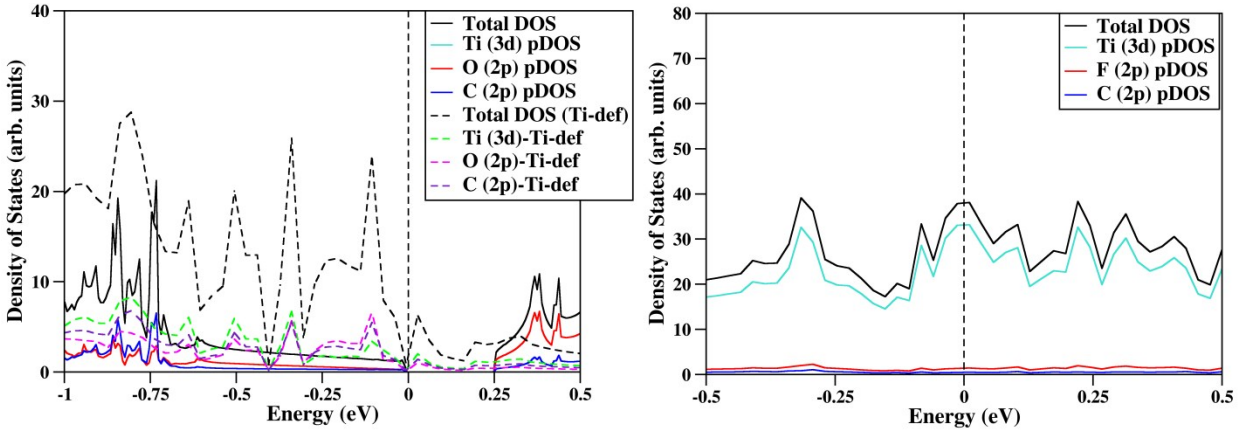

Figure S8: Projected density of states (pDOS) plot for Ti_2CO_2/ V_{Ti}-Ti_2CO_2 and Ti_2CF_2, showing a presence of only fractional and negligible amount of d-electrons on Ti in Ti_2CO_2/V_{Ti}-Ti_2CO_2.

References:

[1] M. Naguib, J. Halim, J. Lu, K. M. Cook, L. Hultman, Y. Gogotsi, and M. W. Barsoum, Journal of the American Chemical Society **135**, 15966 (2013).
[2] A. N. Enyashin and A. L. Ivanovskii, The Journal of Physical Chemistry C **117**, 13637 (2013).
[3] J. He, P. Lyu, and P. Nachtigall, Journal of Materials Chemistry C **4**, 11143 (2016).
[4] S Nosé, The Journal of chemical physics **81**, 511 (1984).
[5] W. G. Hoover, Physical Review A **31**, 1695 (1985).
[6] S. Nosé, The Journal of chemical physics **81**, 511 (1984).